

AUTOMATIC REGIONS OF INTEREST IN FACTOR ANALYSIS FOR DYNAMIC MEDICAL IMAGING

Václav Šmídl, Ondřej Tichý

Institute of Information Theory and Automation,
Pod vodarenskou vezi 4, Prague 8, Czech republic,
smidl@utia.cas.cz, otichy@utia.cas.cz

ABSTRACT

Factor Analysis (FA) is a well established method for factors separation in analysis of dynamic medical imaging. However, its assumptions are valid only in limited regions of interest (ROI) in the images which must be selected manually or using heuristics. The resulting quality of separation is sensitive to the choice of these ROI. We propose a new probabilistic model for functional analysis with inherent estimation of probabilistic ROI. The model is solved using the Variational Bayes method which provides also automatic relevance determination of the estimated factors. Performance of the method is demonstrated on data from renal scintigraphy, where a significant improvement is achieved. Since there are no scintigraphy-related assumptions, the method can be used in any other imaging modality.

Index Terms—Blind Source Separation, Dynamic Imaging, Factor Analysis, Regions of Interest, Renal Scintigraphy

1. INTRODUCTION

Factor Analysis (FA) is a method of Blind Source Separation (BSS) that is widely used in analysis of dynamic medical sequences where a superposition of biological factors is observed. FA models the image sequence as a linear combination of the factor images weighed by their time activity curves. The factor is then composed from one factor image and its time activity curve. The method has been used in many modalities, such as functional Magnetic Resonance Imaging (fMRI) [1], Positron Emission Tomography (PET) [2], or Scintigraphy [3].

The assumptions of linear combinations are typically not valid over the full size of the images but only in a limited area. This problem is typically approached by defining regions of interest (ROI) in the sequence where the assumptions are justified and the factor analysis yields much better results [4]. This can be done either manually, or using some existing segmentation method, [5]. In clinical practice, the ROI selection is almost exclusively done by specialists, since consequences of the ROI for the subsequent factor analysis must be carefully examined. Often, the ROI must be selected iteratively

until an acceptable solution is found. This procedure is very time consuming and strongly depends on the experience of the specialists [3].

In many approaches, FA and ROI selection are viewed as two independent steps, the role of the ROI selection is considered as a preprocessing step for the FA. In this contribution, we propose to combine these two steps in a single probabilistic model, where the factors and the ROI are parameters of the model. Solution of this model is found using the Variational Bayes method [6] which results in an iterative algorithm where FA and automatic ROI selection are iterated until convergence.

As an example, we demonstrate the new model in planar dynamic scintigraphy image sequence.

2. VARIATIONAL FACTOR ANALYSIS

The objective is to analyze a sequence of n images obtained at time $t = 1, \dots, n$ and stored in vectors \mathbf{d}_t with pixels stacked columnwise. The number of pixels in each image is p , thus $\mathbf{d}_t \in \mathbf{R}^p$. The important assumption is that every observed image is a linear combination of r factor images, stored in vectors $\mathbf{a}_j \in \mathbf{R}^p$, $j \in 1, \dots, r$, using the same order of pixels as in \mathbf{d}_t . The dimensions of the problem are typically ordered as $r < n \ll p$. Each factor image has its respective time-activity curve stored in vector $\mathbf{x}_j \in \mathbf{R}^n$, $j \in 1, \dots, r$, $\mathbf{x}_j = [x_{1,j}, \dots, x_{n,j}]'$, \mathbf{x}' denotes transpose of vector \mathbf{x} . With these assumptions, the model of Factor Analysis is:

$$\mathbf{d}_t = \sum_{j=1}^r \mathbf{a}_j x_{t,j} + \mathbf{e}_t, \quad (1)$$

where vector \mathbf{e}_t denotes the noise of the t -th observed image. Note that all vectors $\mathbf{a}_{j \in 1, \dots, r}$, $\mathbf{x}_{j \in 1, \dots, r}$, $\mathbf{e}_{t \in 1, \dots, n}$ are unknown and must be estimated from measurements $\mathbf{d}_{t \in 1, \dots, n}$.

Additional biologically-motivated assumptions are imposed on the elements of the probabilistic model of FA (1): (i) all elements of the observed vectors $\mathbf{d}_{t \in 1, \dots, n}$ are positive, (ii) all elements of the factor images $\mathbf{a}_{j \in 1, \dots, r}$ and the factor curves $\mathbf{x}_{j \in 1, \dots, r}$ are also positive, and (iii) the number of relevant factors, r , is unknown. These assumptions are translated

into probabilistic model as follows [6]

$$f(\mathbf{d}_t|\mathbf{a}, \mathbf{x}, \omega) = \text{tN}_{\mathbf{d}_t} \left(\sum_{j=1}^r \mathbf{a}_j x_{t,j}, \omega^{-1} I_p \right), \quad (2)$$

$$f(\omega) = G_{\omega}(\vartheta_0, \rho_0), \quad (3)$$

$$f(\mathbf{x}_j|v_j) = \text{tN}_{\mathbf{x}_j}(\mathbf{0}_n, v_j^{-1} I_n), \quad (4)$$

$$f(v_j) = G_{v_j}(\alpha_j, 0, \beta_j, 0), \quad (5)$$

$$f(\mathbf{a}_j) = \text{tN}_{\mathbf{a}_j}(\mathbf{0}_p, I_p), \quad (6)$$

where $f(\cdot|\cdot)$ denotes conditional probability density, $\text{tN}(\cdot, \cdot)$ is the positive truncated normal distribution, I_n is an identity matrix of size n , $G(\cdot, \cdot)$ is the gamma distribution, and $\mathbf{0}_n$ is a vector of zeros of size n . Here, $\omega \in \mathbf{R}$ is the parameter of the inverse noise variance, and $v = [v_1, \dots, v_r]' \in \mathbf{R}^r$ is a vector with hyperparameters modeling prior variance of each factor. This parameter is crucial in the Automatic Relevance Determination (ARD) procedure [7]. Parameters $\vartheta_0 \in \mathbf{R}$, $\rho_0 \in \mathbf{R}$, $\alpha_0 \in \mathbf{R}^r$, and $\beta_0 \in \mathbf{R}^r$ are prior parameters of the model that has to be selected.

This probabilistic model is solved using Variational Bayes (VB) method [6] and the solution is found in the form of posterior probability densities of the same type as in (3)–(6) but with different shaping parameters. Equations for the posterior shaping parameters form an implicit set which has to be solved iteratively. The iterative algorithm is proven to converge to a local minimum, see [6] for details. This approach will be denoted as the FA algorithm.

Variational FA is closely related to the Independent Component Analysis, the method for Blind Source Separation, see [8].

An illustrative example of its results is in Fig. 2. The results indicate incomplete separation of the factors due to unrealistic assumptions. Note that the estimated factor images (left column of Fig. 2) affect only a small number of pixels in the full image. However, the model (6) is based on assumption that the j th factor is active in all pixels of the observed area. Therefore, we propose a new model of FA with integrated probabilistic ROI estimation.

3. PROBABILISTIC REGION OF INTERESTS INTEGRATION

The main idea is to decompose the factor image into pixels that belong to the biological factor and those that are zero. Each pixel $\mathbf{a}_{i,j}$ in the factor image \mathbf{a}_j has an indicator variable $\mathbf{i}_{i,j}$ such that

$$\mathbf{i}_{i,j} = \begin{cases} 1 & \text{i-th pixel belongs to the j-th factor} \\ 0 & \text{i-th pixel not belongs to the j-th factor} \end{cases}. \quad (7)$$

These variables are stored in vector \mathbf{i}_j using the same order as pixels in vector \mathbf{a}_j . Formally, we could form a model with discrete variable \mathbf{i}_j , however, solution of such model would

be computationally very costly. Therefore, we relax the assumption (7) using probabilities:

$$f(a_{i,j}) = U(0, 1)^{\mathbf{i}_{i,j}} \text{tN}(0, \xi_j^{-1})^{(1-\mathbf{i}_{i,j})}, \quad (8)$$

$$f(\xi_j) = G_{\xi_j}(\phi_j, \psi_j). \quad (9)$$

where $\mathbf{i}_{i,j}$ is a continuous variable $\mathbf{i}_{i,j} \in \langle 0, 1 \rangle$. Note that (8)–(9) is a soft version of model (7) since it has two extremes

$$f(a_{i,j}) = \begin{cases} U(0, 1) & \mathbf{i}_{i,j} = 1, \\ \text{tN}(0, \xi_j^{-1}) & \mathbf{i}_{i,j} = 0, \end{cases}$$

where for $\mathbf{i}_{i,j} = 0$ the prior is uniform over the whole range of possibilities, and for $\mathbf{i}_{i,j} = 1$ the prior is very narrow around 0. Strictness of the requirement of zero for $\mathbf{i}_{i,j}$ is governed by unknown parameter ξ_j .

Following the Variational Bayes methodology, we select prior for the $\mathbf{i}_{i,j}$ variable using the principle of VB conjugacy [6]. The prior is then

$$f(\mathbf{i}_{i,j}) = \text{tExp}(\lambda_{i,j,0}, (0, 1]), \quad (10)$$

where $\text{tExp}(\lambda, (a, b])$ is exponential distribution with parameter λ truncated between interval $(a, b]$ and $\lambda_{i,j,0}$ a prior chosen parameter. Hence, \mathbf{i}_j is the probabilistic ROI of the image \mathbf{a}_j .

3.1. Variational Solution

The new model of FA is given by equations from Section 2, (2)–(5), and new model of factor images, (8)–(10). We solve this model using the VB method yielding the following posterior densities:

$$f(\mathbf{x}_j|\mathbf{d}, r) = \text{tN}_{\mathbf{x}_j}(\mu_{\mathbf{x}_j}, \Sigma_{\mathbf{x}_j}), \quad (11)$$

$$f(v_j|\mathbf{d}, r) = G_{v_j}(\alpha_j, \beta_j), \quad (12)$$

$$f(\omega|\mathbf{d}, r) = G_{\omega}(\vartheta, \rho), \quad (13)$$

$$f(\mathbf{a}_i|\mathbf{d}, r) = \text{tN}_{\mathbf{a}_i}(\mu_{\mathbf{a}_i}, \Sigma_{\mathbf{a}_i}), \quad (14)$$

$$f(\xi_j|\mathbf{d}, r) = G_{\xi_j}(\phi_j, \psi_j), \quad (15)$$

$$f(\mathbf{i}_{i,j}|\mathbf{d}, r) = \text{tExp}_{\mathbf{i}_{i,j}}(\lambda_{i,j}, (0, 1]). \quad (16)$$

Note that the vector \mathbf{a}_i is the vector with i -th pixel decomposition, $\mathbf{a}_i = [a_{i,1}, \dots, a_{i,r}]'$. The shaping parameters $\mu_{\mathbf{x}_j}, \Sigma_{\mathbf{x}_j}, \alpha_j, \beta_j, \vartheta, \rho, \mu_{\mathbf{a}_i}, \Sigma_{\mathbf{a}_i}, \phi_j, \psi_j, \lambda_{i,j}$ of distributions (11)–(16) are given in Appendix A. The order of calculation scheme is shown in Fig. 1. We call this algorithm as the FA with probabilistic ROI (FAROI) algorithm.

In the following text, we denote the estimates of the parameter as $\langle \cdot \rangle$, e.g. $\langle \mathbf{a}_j \rangle$ or $\langle \mathbf{x}_j \rangle$.

4. EXPERIMENT: RENAL SCINTIGRAPHY DATA

In this Section, we apply methodologies from Sections 2 and 3 to a clinical data set from renal scintigraphy. At first, we briefly revise scintigraphy and biological assumptions on dynamics of kidneys.

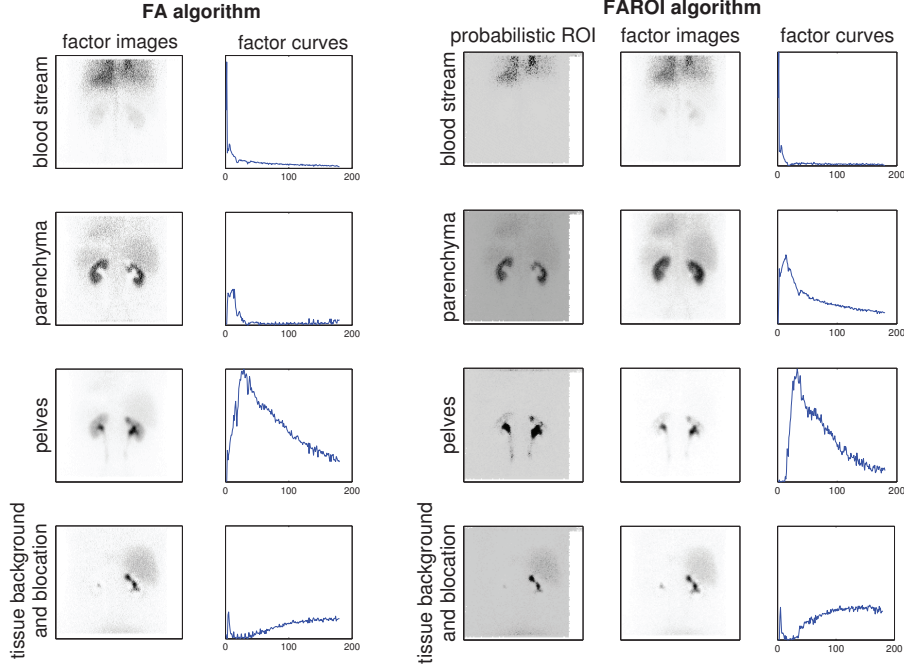


Fig. 2. Results from FA and FAROI algorithms. Left: results of the FA alg. left-to-right: factor images, $\langle \mathbf{a}_j \rangle$, and factor curves, $\langle \mathbf{x}_j \rangle$. Right: results of the FAROI alg. left-to-right: probabilistic ROI, $\langle \mathbf{i}_j \rangle$, factor images, $\langle \mathbf{a}_j \rangle$, and factor curves, $\langle \mathbf{x}_j \rangle$.

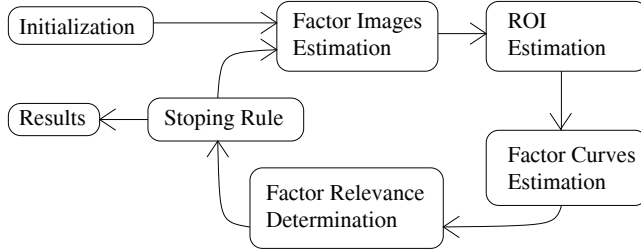


Fig. 1. The computation scheme of the FAROI algorithm.

4.1. Renal Scintigraphy

Scintigraphy is a well established and important diagnostic method in nuclear medicine. We are concerned with planar dynamic scintigraphy where the measurements are in the form of a sequence of images of the same scanned region of a body. Each pixel in the sequence is a summation of radioactive particles incoming from a volume of body under the detector. Therefore, each pixel accumulates activity from potentially many factors. The factors has to be separated using a source separation method such as factor analysis.

A healthy kidney is composed of two main structures, parenchyma and pelvis. There are two important specific properties of these data: (i) the parenchyma is typically surrounding the whole pelvis, and (ii) at the first 100 – 180 seconds (depending on the patient’s state) only the parenchyma is active [9]; after this time, the activity passes from parenchyma

through pelvis to urinary bladder. This time-parameter is important diagnostical coefficient and will be denoted as the Parenchymal Transit Time (PTT). If this assumptions are not satisfied, the factor separation is incomplete and could cause significant error in diagnostics. There could be some exceptions in case of abnormal or harmed kidney, this case must be carefully considered by the physicians.

4.2. Experiment

Algorithms derived in Sections 2 and 3 were applied on a representative clinical set of dynamic renal scintigraphy. The sequence contains 180 images taken after each 10 seconds. The size of each image is 128×128 pixels. The scanned region contains heart, lungs, kidneys, and other organs in the background.

In both algorithms, only four factors were found to be relevant by the ARD, section 2. These are shown in Fig. 2, for the FA algorithm (left) and for the FAROI algorithm (right). Both algorithms estimate the same biological organs (from the top): blood background, parenchyma, pelvis, and tissue background mixed with some blockage in the right kidney.

The main differences between the results of the algorithms are in the second and the third factors, parenchyma and pelvis. Parenchyma obtained from the FA algorithm has abnormally over-subtracted areas where the pelvis are active; as a result, the time activity curve does not have the shape typical for a parenchyma. The estimates of the parenchyma

factor image and its time activity curve from FAROI algorithm do not suffer from such degradation and are biologically correct.

The estimate of the pelvis image obtained from the FA algorithm is corrupted by addition of pixels from the parenchyma. Therefore, its time activity curve starts immediately and not after at least 100 seconds. The estimates provided by the FAROI algorithm much better localize the pelvis and exhibit zero time activity in the first 120 seconds from which it is easy to estimate the corresponding PPT.

Due to increase in complexity, the FAROI algorithm is approximately 3 times more time-consuming than the FA algorithm. However, evaluation of both algorithms is in order of minutes on a contemporary PC.

5. CONCLUSION AND DISCUSSION

A new probabilistic model for analysis of dynamic image sequence is proposed. The main extension of the factor analysis model is a parameter representing regions of interest for each factor. This encodes the elementary knowledge that the factors do not cover full area of the picture. The Variational Bayes method was applied to obtain estimates of all unknown model parameters.

Preliminary experiments with the FAROI algorithm indicate that the extension is well justified and has significant impact on realistic estimates of the biological factors. Specifically, the new model is capable of better separation of the factors which leads to easier evaluation of diagnostic coefficients. For example, the coefficient of parenchymal transit time can be now easily recognized in the resulting factor curve which was not possible with the factor analysis model. However, an extensive comparative study will be necessary for clinical verification of the algorithm.

The assumptions of the new model are not unique to scintigraphy, hence the resulting algorithm can be applied in any modality.

Acknowledgement: We thank Prof. M. Šámal from the First Faculty of Medicine, Charles University in Prague for his support and provided data.

6. REFERENCES

[1] K. Van Leemput, F. Maes, D. Vandermeulen, and P. Suetens, “Automated model-based bias field correction of MR images of the brain,” *Medical Imaging, IEEE Transactions on*, vol. 18, no. 10, pp. 885–896, 1999.

[2] G. El Fakhri, A. Sitek, B. Guérin, M.F. Kijewski, M.F. Di Carli, and S.C. Moore, “Quantitative dynamic cardiac 82rb pet using generalized factor and compartment analyses,” *Journal of Nuclear Medicine*, vol. 46, no. 8, pp. 1264, 2005.

[3] M. Caglar, G.K. Gedik, and E. Karabulut, “Differential renal function estimation by dynamic renal scintigraphy: influence of background definition and radiopharmaceutical,” *Nuclear medicine communications*, vol. 29, no. 11, pp. 1002, 2008.

[4] G.P. Liney, P. Gibbs, C. Hayes, M.O. Leach, and L.W. Turnbull, “Dynamic contrast-enhanced mri in the differentiation of breast tumors: User-defined versus semi-automated region-of-interest analysis,” *Journal of Magnetic Resonance Imaging*, vol. 10, no. 6, pp. 945–949, 1999.

[5] N. Michoux, JP Vallee, A. Pechere-Bertschi, X. Montet, L. Buehler, and BE Van Beers, “Analysis of contrast-enhanced mr images to assess renal function,” *Magnetic Resonance Materials in Physics, Biology and Medicine*, vol. 19, no. 4, pp. 167–179, 2006.

[6] V. Šmídl and A. Quinn, *The Variational Bayes Method in Signal Processing*, Springer, 2005.

[7] C.M. Bishop and M.E. Tipping, “Variational relevance vector machines,” in *Proceedings of the 16th Conference on Uncertainty in Artificial Intelligence*. San Francisco: Morgan Kaufmann Publishers, 2000, pp. 46–53.

[8] J.W. Miskin, *Ensemble learning for independent component analysis*, Ph.D. thesis, University of Cambridge, 2000.

[9] E. Durand, M.D. Blaufox, K.E. Britton, O. Carlsen, P. Cosgriff, E. Fine, J. Fleming, C. Nimmon, A. Piepsz, A. Prigent, et al., “International Scientific Committee of Radionuclides in Nephrourology (ISCORN) consensus on renal transit time measurements,” in *Seminars in nuclear medicine*. Elsevier, 2008, vol. 38, pp. 82–102.

A. SHAPING PARAMETERS OF POSTERIOR DENSITIES

Note that the results are in matrix form, e.g. $A = [a_1, \dots, a_r]$, in the appendix. Shaping parameters of posterior densities (11) - (16) are given as $\Sigma_X^{-1} = \langle \omega \rangle \langle A' A \rangle + \text{diag}(\langle v \rangle)$, $\mu_X = \langle \omega \rangle D' \langle A \rangle \Sigma_X$, $\alpha = \alpha_0 + \frac{n}{2} \mathbf{1}_{r,1}$, $\beta = \beta_0 + \frac{1}{2} \text{diag}(\langle X' X \rangle)$, $\vartheta = \vartheta_0 + \frac{pn}{2}$, $\rho = \rho_0 + \frac{1}{2} \text{tr}(DD' - \langle A \rangle \langle X' \rangle D' - D \langle X \rangle \langle A' \rangle + \langle A' A \rangle \langle X' X \rangle)$, $\Sigma_{a_i}^{-1} = \langle \omega \rangle \sum_{k=1}^n \langle x'_k x_k \rangle + \langle \xi \rangle (I_r - \text{diag}(\mathbf{i}_i))$, $\mu'_{a_i} = \Sigma_{a_i} \langle \omega \rangle \sum_{k=1}^n (\langle x_k \rangle D_{i,k})'$, $\phi_j = \phi_{j,0} + \frac{1}{2} \sum_{i=1}^p (1 - \langle \mathbf{i}_{i,j} \rangle)$, $\psi_j = \psi_{j,0} + \frac{1}{2} \sum_{i=1}^p (1 - \langle \mathbf{i}_{i,j} \rangle) \langle a_{i,j}^2 \rangle$, $\lambda_{i,j} = \lambda_{i,j,0} - \frac{1}{2} \langle \ln \xi_j \rangle + \frac{1}{2} \langle a_{i,j} \xi_j a_{i,j} \rangle$, where $\text{tr}(\cdot)$ is a trace of the argument, $\text{diag}(\cdot)$ denotes (i) a square matrix with argument vector on diagonal and zeros otherwise or (ii) a vector composed from diagonal element of argument matrix, and $\mathbf{1}_{r,1}$ denotes vectors of ones of respective size. The required moments are given as $\langle v_i \rangle = \alpha_i \beta_i^{-1}$, $\langle \xi_i \rangle = \phi_i \psi_i^{-1}$, $\langle \omega \rangle = \vartheta \rho^{-1}$, $\langle \mathbf{i}_{i,j} \rangle = \lambda_{i,j}^{-1}$ and moments of truncated normal distribution are given e.g. in [6].